IEEJ Journal of Industry Applications
Vol.6 No.6 pp.429–434 DOI: 10.1541/ieejjia.6.429

Paper

Instantaneous Vector Control of Four Switch Three Phase Inverter Fed Induction Motor Drive

Ufot Ufot Ekong[*a)] Student Member, Mamiko Inamori[*] Member
Masayuki Morimoto[*] Fellow

(Manuscript received Jan. 23, 2017, revised May 25, 2017)

This paper proposes a transformation matrix to generate two phase reference voltage signals for Four Switch Three Phase Inverter (FSTPI) using vector control. The feasibility of the control strategy is verified by proving the power invariance before and after the transformation. Simulation and experimental results have verified the validity and effectiveness of the proposed method to obtain instantaneous response in different operating conditions and provide fast speed response.

Keywords: emergency drive, electric vehicles, field oriented control, torque, two phase inverter, transformation matrix

1. Introduction

Pulse Width Modulation (PWM) voltage source inverter fed induction motor drives are widely used from consumer products to industrial applications. Much research has been conducted on Four Switch Three Phase Inverter (FSTPI) [(1)–(19)]. Some of these researches have proposed FSTPI to reduce cost [(1)(2)], others as an emergency drive during inverter failure of the conventional three phase inverter [(3)(4)].

Prior work performed on FSTPI focused on the Space Vector PWM (SVPWM) method to generate signals for FSTPI have been reported. Three kinds of space vector modulation techniques that made the voltage vector track a desired circular trajectory was proposed in (5). The same author also extended his previous work by compensating the voltage error [(6)]. Various space vector modulation strategies have also been proposed to compensate the voltage errors caused by the DC-link center tap voltage fluctuation [(7)–(11)].

SVPWM has been reported to offer good dynamic performance and reduction in torque ripple [(12)]. Furthermore, SVPWM applied to an FSTPI drive experiences modulation and unbalanced current problems, of which compensation techniques are proposed [(13)(14)]. Nevertheless, in order to implement this control method, complex algorithms are required. These algorithms require high performance controllers for heavy calculations and, in some cases, increase the cost of the drive [(15)]. SVPWM fed FSTPI drive has also been reported to have limitations with implementation because a different strategy is required depending on the affected phase of the inverter. Therefore, 3 different startegies must be prepared which will take up lots of memory space in the controller [(16)].

A less complicated method and easily implementable method of generating signals is still required. In order to realize this objective a sinusoidal PWM technique in time domain is a preferable method. To date, no paper has considered or developed a method to generate sinusoidal PWM for FSTPI.

Earlier results using the conventional open loop volts per hertz (V/F) control system, reported an inadequacy of torque at low speed regions [(17)]. In order to apply Four Switch Three Phase Inverter to high performance motor drives that require full torque at low speed regions, a control method that can produce full torque at zero speed is required.

Previous work, analyzed that FSTPI drive using vector control can achieve a three phase balanced current [(18)]. However, no paper has reported information on the torque characteristics of Four Switch Three Phase Inverter using coordinate transformation algorithm.

In this paper, a new transformation matrix to generate sinusoidal PWM signals for FSTPI in time domain is proposed. Design strategy, some simulation and experimental results including torque characteristics of the FSTPI drive using vector control will be presented and discussed.

2. Four Switch Three Phase Inverter

2.1 Structure of Four Switch Three Phase Inverter

The circuit of FSTPI is shown in Fig. 1. FSTPI consists of four switches, A and B phases are connected to the U and W phases of the induction motor respectively. The V phase of the motor is connected to the center potential of the DC source.

2.2 Principle of Four Switch Three Phase Inverter

The V connection of a three phase circuit is shown in Fig. 2. As shown in Eq. (1), V_A and V_B are the AC power source which has a phase difference of $\pi/3$. When these two phase power supply voltage (V_A, V_B) is applied to a three phase load, a three phase balanced voltage V_{un}, V_{vn} and V_{wn}, is generated as shown in Eq. (2). Therefore, it can been seen that a two phase AC power supply with a phase difference of $\pi/3$ can drive a three phase motor. This is the basic working principle of an FSTPI drive.

a) Correspondence to: Ufot Ufot Ekong. Email: 6ltad001@mail.u-tokai.ac.jp
* Tokai University
4-1-1, Kitakaname, Hiratsuka, Kanagawa 259-1292, Japan

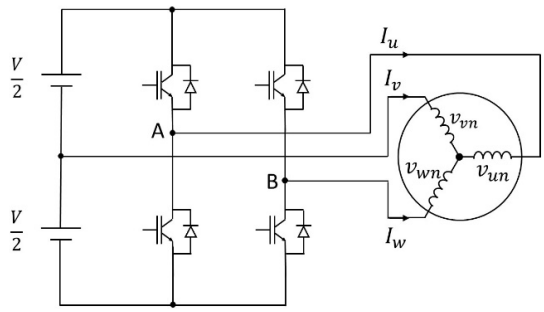

Fig. 1. Structure of Four Switch Three Phase Inverter Circuit

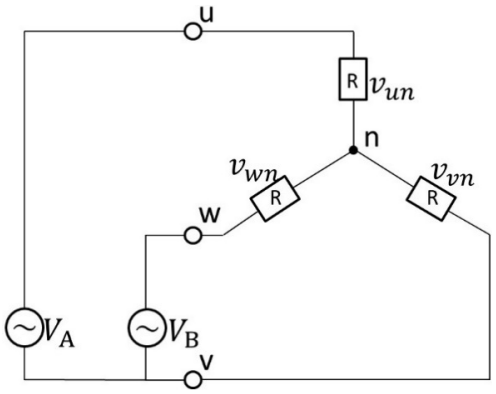

Fig. 2. Four Switch Three Phase Inverter Power circuit

$$V_A = V \cdot \sin \omega t$$
$$V_B = V \cdot \sin\left(\omega t + \frac{\pi}{3}\right) \quad \cdots\cdots (1)$$
$$V_{un} = \frac{1}{\sqrt{3}} V \cos\left(\omega t - \frac{\pi}{6}\right)$$
$$V_{vn} = \frac{1}{\sqrt{3}} V \cos\left(\omega t - \frac{5\pi}{6}\right) \quad \cdots\cdots (2)$$
$$V_{wn} = \frac{1}{\sqrt{3}} V \cos\left(\omega t + \frac{\pi}{2}\right)$$

3. Sinusoidal PWM Technique for FSTPI

In the Control strategy of the conventional vector control fed three phase inverter motor drive, a three phase sinusoidal reference voltage V_u, V_v, V_w is generated. Since vector control is conducted in dq axis, the output voltage reference is V_d, V_q, which is transformed into voltage vector axis ($\alpha\beta$) using inverse park transformation to V_α, V_β as shown in Eqs. (3) and (4). This voltage vector (V_α, V_β) is then transformed using inverse Clarke transformation to a sinusoidal 3 phase reference voltage (V_u, V_v, V_w) used to generate PWM signals for the inverter as shown in Eqs. (5) and (6).

In the two phase $\alpha\beta$ axis to UVW axis transformation, a constant K = $\sqrt{2/3}$ is multiplied in order to retain the same power before and after the transformation. The following condition are also required for the transformation; $\theta = \omega t$, $V_d = \sqrt{3}V$, $V_q = 0$.

$$\begin{bmatrix} V_\alpha \\ V_\beta \end{bmatrix} = \begin{bmatrix} \cos\theta & -\sin\theta \\ \sin\theta & \cos\theta \end{bmatrix} \begin{bmatrix} V_d \\ V_q \end{bmatrix} \quad \cdots\cdots (3)$$
$$V_\alpha = \sqrt{3}V \cos \omega t$$
$$V_\beta = \sqrt{3}V \sin \omega t \quad \cdots\cdots (4)$$

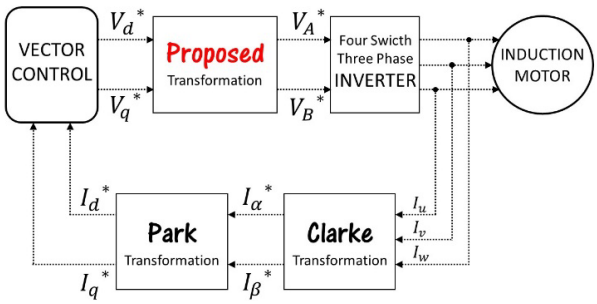

Fig. 3. Block diagram of the proposed system

$$\begin{bmatrix} V_u \\ V_v \\ V_w \end{bmatrix} = \sqrt{\frac{2}{3}} \begin{bmatrix} \cos 0 & \sin 0 \\ \cos\frac{2}{3}\pi & \sin\frac{2}{3}\pi \\ \cos\frac{4}{3}\pi & \sin\frac{4}{3}\pi \end{bmatrix} \begin{bmatrix} V_\alpha \\ V_\beta \end{bmatrix} \quad \cdots\cdots (5)$$
$$V_u = \sqrt{2}V \cos \omega t$$
$$V_v = \sqrt{2}V \cos\left(\omega t - \frac{2}{3}\pi\right) \quad \cdots\cdots (6)$$
$$V_w = \sqrt{2}V \cos\left(\omega t - \frac{4}{3}\pi\right)$$

3.1 Proposed Control Strategy The block diagram of the proposed system is shown in Fig. 3. In the case of FSTPI, a two phase voltage reference that has a phase difference of $\pi/3$ is required to generate PWM signals. In this paper a new transformation matrix is proposed to generate signals for FSTPI by creating a transformation matrix.

The proposed transformation matrix is shown in Eq. (7). The matrix is applied to the two phase voltage vector reference (V_d, V_q) to transform the signals into a two phase scalar reference voltage (V_A, V_B) as shown in Eq. (8). In this new transformation matrix, a constant K = $\sqrt{2/3}$ is also required to facilitate power invariance of the transformation. The following condition are also required for the transformation; $\theta = \omega t$, $V_d = \sqrt{3}V$, $V_q = 0$.

$$\begin{bmatrix} V_A \\ V_B \end{bmatrix} = \sqrt{\frac{2}{3}} \begin{bmatrix} \cos\theta & -\sin\theta \\ \cos\left(\theta + \frac{\pi}{3}\right) & \sin\left(\theta - \frac{2}{3}\pi\right) \end{bmatrix} \begin{bmatrix} V_d \\ V_q \end{bmatrix} \cdots (7)$$
$$V_A = \sqrt{\frac{2}{3}} \left(V_d \cos\theta - V_q \sin\theta\right)$$
$$V_B = \sqrt{\frac{2}{3}} \left\{ V_d \cos\left(\theta + \frac{\pi}{3}\right) + V_q \sin\left(\theta - \frac{2}{3}\pi\right) \right\} \cdots (8)$$
$$V_A^* = \sqrt{2}V \cos \omega t$$
$$V_B^* = \sqrt{2}V \cos\left(\omega t + \frac{\pi}{3}\right) \cdots\cdots (9)$$

The reference voltage (V_A^*, V_B^*) in Eq. (9) is a sinusoidal waveform of the same amplitude but with a phase difference of $\pi/3$. This reference voltage can be used to generate PWM signals to drive the FSTPI.

3.2 Power Invariance In order to mathematically validate the proposed transformation matrix, the power invariance is calculated. Power invariance indicates that the power before and after the transformation is the same. The global condition to prove power invariance before and after transformation is shown below in Eq. (10). Where [C] is the

proposed transformation matrix, $[C]^{-1}$ is the inverse of the proposed matrix and $[C]^{t}$ is the transposed matrix.

In order to calculate power invariance, the proposed transformation matrix [C] in Eq. (7) must be a three rows and three columns matrix. Therefore, the transformation matrix axis is rewritten as V_{dq0} to V_{AB0} as shown in Eq. (11). From the calculation results, Eqs. (13) and (14) are the same, this proves the power invariance of the proposed transformation matrix.

$$[C]^{-1} = [C]^{t}. \quad \cdots\cdots (10)$$

$$\begin{bmatrix} V_A \\ V_B \\ V_0 \end{bmatrix} = \sqrt{\frac{2}{3}} \begin{bmatrix} \cos\theta & -\sin\theta & \frac{1}{\sqrt{2}} \\ \cos\left(\theta+\frac{\pi}{3}\right) & \sin\left(\theta-\frac{2}{3}\pi\right) & -\frac{1}{\sqrt{2}} \\ \cos\left(\theta-\frac{\pi}{3}\right) & \sin\left(\theta+\frac{2}{3}\pi\right) & -\frac{1}{\sqrt{2}} \end{bmatrix} \begin{bmatrix} V_d \\ V_q \\ V_0 \end{bmatrix} \quad \cdots\cdots (11)$$

$$[C] = \sqrt{\frac{2}{3}} \begin{bmatrix} \cos\theta & -\sin\theta & \frac{1}{\sqrt{2}} \\ \cos\left(\theta+\frac{\pi}{3}\right) & \sin\left(\theta-\frac{2}{3}\pi\right) & -\frac{1}{\sqrt{2}} \\ \cos\left(\theta-\frac{\pi}{3}\right) & \sin\left(\theta+\frac{2}{3}\pi\right) & -\frac{1}{\sqrt{2}} \end{bmatrix} \quad \cdots\cdots (12)$$

$$[C]^{-1} = \sqrt{\frac{2}{3}} \begin{bmatrix} \cos\theta & \cos\left(\theta+\frac{\pi}{3}\right) & \cos\left(\theta-\frac{\pi}{3}\right) \\ -\sin\theta & \sin\left(\theta-\frac{2}{3}\pi\right) & \sin\left(\theta+\frac{2}{3}\pi\right) \\ \frac{1}{\sqrt{2}} & -\frac{1}{\sqrt{2}} & -\frac{1}{\sqrt{2}} \end{bmatrix} \quad \cdots\cdots (13)$$

$$[C]^{t} = \sqrt{\frac{2}{3}} \begin{bmatrix} \cos\theta & \cos\left(\theta+\frac{\pi}{3}\right) & \cos\left(\theta-\frac{\pi}{3}\right) \\ -\sin\theta & \sin\left(\theta-\frac{2}{3}\pi\right) & \sin\left(\theta+\frac{2}{3}\pi\right) \\ \frac{1}{\sqrt{2}} & -\frac{1}{\sqrt{2}} & -\frac{1}{\sqrt{2}} \end{bmatrix} \quad \cdots\cdots (14)$$

$\therefore [C]^{-1} = [C]^{t}$

4. Vector Control

Vector control is a control procedure for operating an induction motor that results in fast dynamic response and energy efficient operations at all speeds. It maintains high efficiency over a wide range and allows for precise dynamic control of speed and torque.

The block diagram of a vector control fed FSTPI drive is shown in Fig. 4 and its basic equations are given below (15)–(18). Vector control accomplishes instantaneous commutation with velocity feedback from the motor ω_r and a feed forward slip command ω_s. The stator current of the motor current is decomposed into magnetizing (flux producing) component I_d and torque component I_q. These components are then decoupled and controlled individually. The magnetizing component I_d, varies slowly and is kept constant for fast response. As shown in Fig. 4, the speed, I_d and I_q reference is compared to the feedback value and the error is processed through a PI controller. The output command after vector control V_d, V_q is transformed to two phase voltage reference signal V_A, V_B. This reference signal is used to generate PWM signals by the inverter and finally transmitted to the motor.

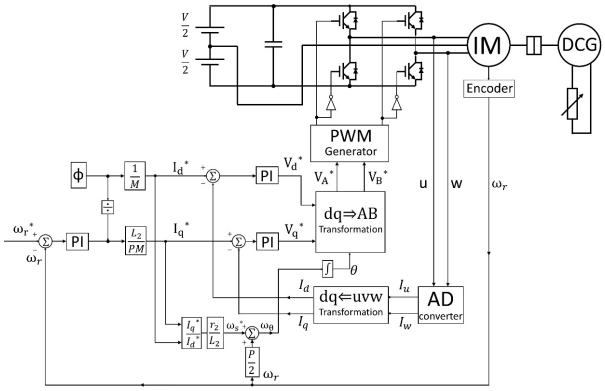

Fig. 4. Vector control block diagram for FSTPI

Table 1. Motor and Inverter Parameters

Induction Motor	Rated Power	p	200	[W]
	Rated Frequency	f	50	[Hz]
	Rated Speed	n	1250	[rpm]
	Rated Torque	T	1.49	[Nm]
	Rated Voltage	*Vline-line*	200	[V]
	Rated Current	I	1.1	[A]
	Number of poles	P	4	[poles]
Inverter	DC link voltage	V	283	[V]
	Filter Capacitor	C	8200	[μF]
	Carrier Frequency	fc	5	[kHz]
	Dead Time	DT	3.5	[μs]

$$I_d^{*} = \frac{\varphi_2}{M} \quad \cdots\cdots (15)$$

$$I_q^{*} = \frac{L_2 T^{*}}{PM\varphi_2^{*}} \quad \cdots\cdots (16)$$

$$\omega_s^{*} = \frac{Mr_2}{L_2\varphi_2^{*}} I_q \quad \cdots\cdots (17)$$

$$\omega_\theta = \frac{P}{2}\omega_r + \omega_s \quad \cdots\cdots (18)$$

5. Simulation Results

To verify the proposed control strategy, a simulation model for FSTPI is designed and implemented. PSIM software is used for the simulation. The main circuit consists of four IGBT switches. In the analysis, the inverter switches are considered as ideal switches. The V phase is assumed to be broken down and connected to the center potential of the DC source. The specification of the induction motor and inverter parameters are shown in Table 1. The torque command is set from 0–1.49 Nm (0% to 100% of the rated torque).

5.1 Reference Voltage The output reference voltage (V_A, V_B) for the FSTPI during operation at motor speed 400 rpm and load torque 1.49 Nm is shown in Fig. 5. The results show that the voltage reference signals after using the proposed transformation matrix has a phase difference of $\pi/3$.

5.2 Motor Current Waveforms The current waveforms of the motor during operation at 400 rpm and its rated

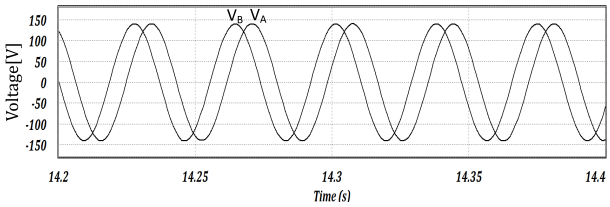

Fig. 5. Voltage Reference (Simulation)

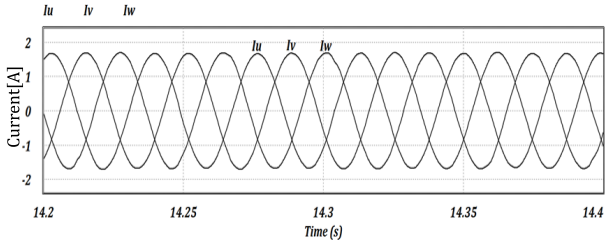

Fig. 6. Motor current waveforms (Simulation)

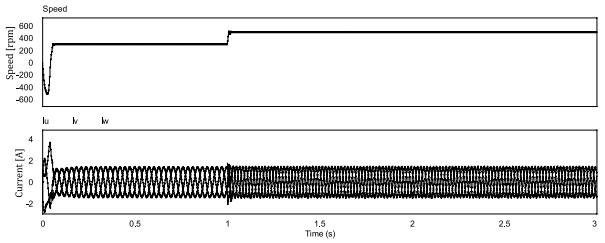

Fig. 7. Speed response (Simulation)

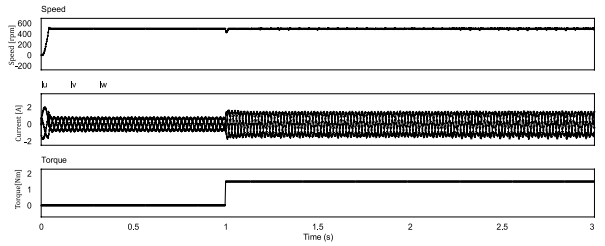

Fig. 8. Instantaneous speed torque response (Simulation)

torque (1.49 Nm) is shown in Fig. 6. The result shows that the three phase current waveforms of the motor are balanced.

5.3 Dynamic Response Characteristics The dynamic response of the system during various speed and load conditions is shown in Fig. 7 and Fig. 8. To examine the response of the drive due to step change in speed, the speed command is increased by 20% at t = 1second from 300 rpm to 500 rpm at full load condition.

Figure 7 shows the motor reaches its command speed in less than a second with negligible oscillations.

The speed and torque response due to increase in load is also examined as shown in Fig. 8. During the start-up operation, the motor speed command is set at 500 rpm and load torque at 0 Nm. After 2 seconds the load torque is stepped up from no load condition to 1.49 Nm (rated torque).

The results show that the motor current amplitude increased in order to handle the increase in torque. Furthermore, when the torque is increased speed slightly falls but recovers in less than a second. These results show the drive has fast dynamic response under different load conditions.

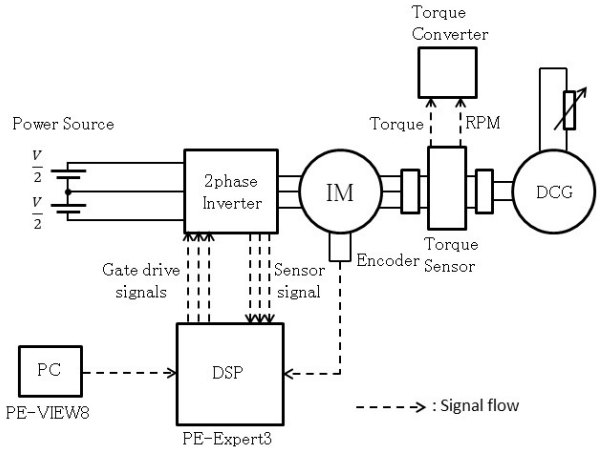

Fig. 9. Experimental System

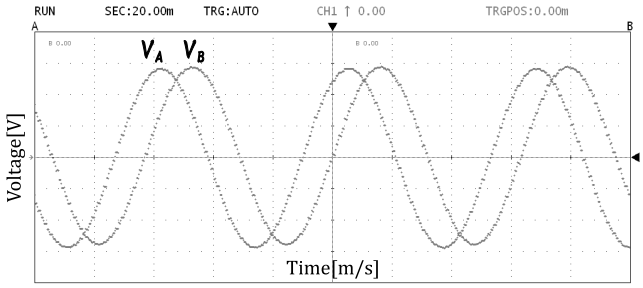

Fig. 10. Voltage Reference (Experiment)

6. Experimental Results

The feasibility of the proposed transformation matrix method for FSTPI is verified by experimental implementation. The same inverter is used for both the two phase and three phase experiments. V phase of the motor is connected to the center potential of the DC source. The specification of the induction motor and the inverter parameters for both two and three phase inverters are shown in Table 1.

The experimental system configuration is shown in Fig. 9. PE-Expert 3 is the digital system which is equipped with a Digital Signal Processor (DSP), Analog Digital (AD) converter and PWM functions. As shown in Fig. 9, the program signals are transmitted from the host computer to the DSP of the PE-Expert3.

6.1 Reference Voltage Figure 10 shows the waveforms of the reference voltage (V_A, V_B) at motor speed 500 rpm and its rated torque 1.49 Nm. The results illustrates the reference voltage has a phase difference of $\pi/3$.

6.2 Motor Current Waveforms The waveform of motor current at speed 500 rpm and rated torque (1.49 Nm) is shown in Fig. 11. The results show the proposed FSTPI drive can achieve a three phase balanced motor current.

6.3 Response Characteristics To evaluate the performance and verify the response characteristics of the proposed control method, the system is tested under different load conditions. The motor speed is set at a constant 500 rpm and the load torque is set from 0–1.49 [Nm].

The response characteristics of the speed and motor currents are shown in Fig. 12. The torque command is increased from 0% to 100% at t = 2 seconds. The results show that as the load torque increases, the motor current amplitude also

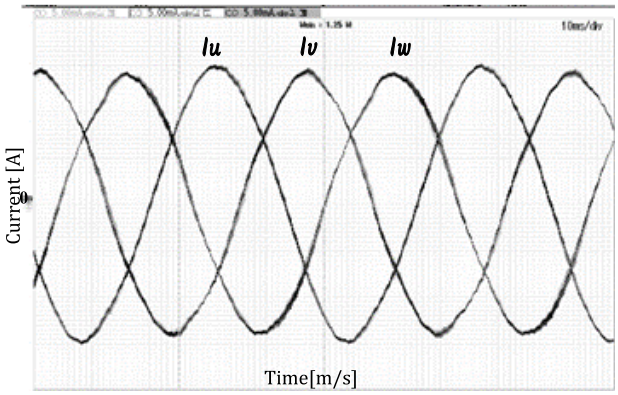

Fig. 11. Three phase motor current waveforms (Experiment)

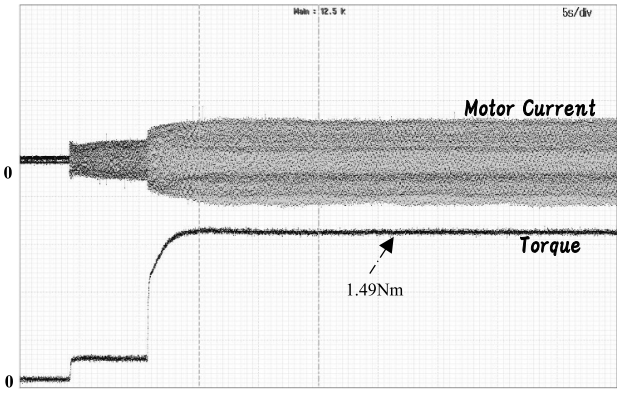

Fig. 12. Instantaneous response of an FSTPI

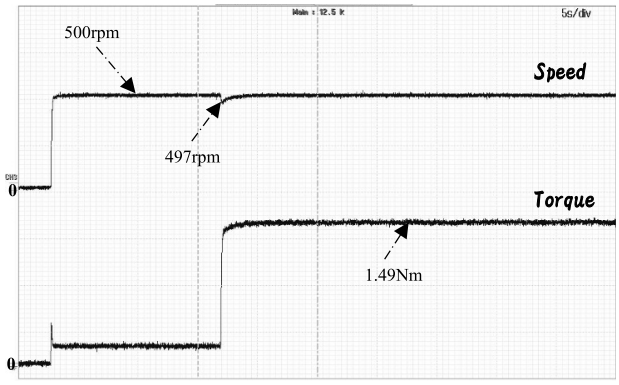

Fig. 13. Speed and Torque response of an FSTPI drive

increases.

Under the same load conditions, the speed response to increase in load torque is shown in Fig. 13. The results show that when the load torque is increased the motor speed slightly falls below the command speed but recovers instantaneously.

Figure 14 illustrates the response of motor speed when the load torque is reduced and increased repeatedly from 1.49 [Nm] to 0 [Nm] and 0 [Nm] to 1.49 [Nm]. The results show that when the load torque is reduced the speed increases slightly above the command speed but returns back to the command speed in less than a second.

Due to Mechanical loss in the experimental system, in a no load condition, when the torque command is set as T = 0 Nm, 0.17 Nm is developed.

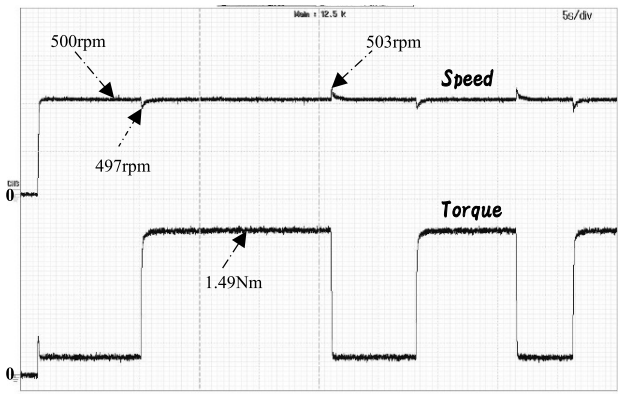

Fig. 14. Instantaneous Torque response of an FSTPI drive

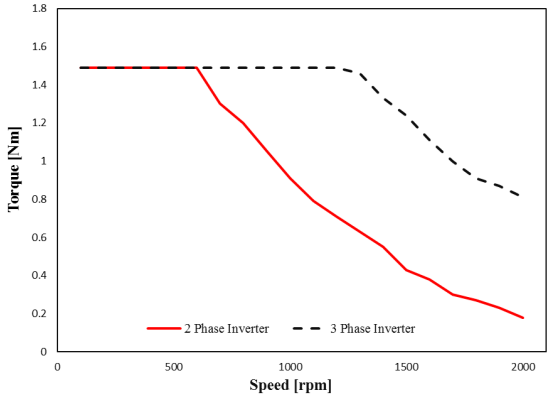

Fig. 15. Torque-speed characteristics of a three-phase induction motor

6.4 Speed-Torque Characteristics The speed torque characteristics of an FSTPI fed induction motor drive is shown in Fig. 15. For comparison purposes, the result of a three phase inverter drive is also shown in Fig. 15. The maximum torque is set at 1.49 Nm (rated value). The experiment results show that;

1. From zero speed region to medium speed region (approx.600 rpm) both in an FSTPI and three phase inverter drive, equivalent torque can be obtained.
2. In the FSTPI drive, maximum torque attainable speed with regard to the torque command (1.49 Nm) reduces above 600 rpm (base speed). However, in a three phase inverter drive, up till 1250 rpm (rated speed), maximum torque can be achieved. Comparing the speed characteristics of an FSTPI and three phase inverter drive, the maximum torque attainable speed reduces by approximately 50%. This is because as shown in Eq. (2), the voltage utilization of an FSTPI compared to a three phase inverter drive reduces by $1/\sqrt{3}$.

7. Conclusions

In this paper, a less complicated and easily implementable control strategy is proposed by creating a transformation matrix to generate PWM signals for FSTPI. The power invariance of the transformation matrix is verified mathematically. The feasibility of the proposed strategy is verified by simulation results and validated by experimental results under

different speed and load conditions. The results obtained and presented in this work indicate that the proposed control method is capable of instantaneous speed and torque response.

Furthermore, this control strategy is suitable for motor drives that require full torque from low speed regions. Further study to improve the speed torque characteristics of an FSTPI drive in high speed regions will be done by proposing a flux weakening control method for Four Switch Three Phase Inverter.

References

(1) G.A. Covic, G.L. Peters, and T. Boys: "An improved single phase to three phase converter for low cost AC motor drives", Proc. IEEE Power Electronics Drives System, pp.549–554 (1995)

(2) H.W.V.D. Broeck and J.D.V. Wyk: "A comparative investigation of a three-phase induction machine drive with a component minimized voltage-fed inverter under different control options", *IEEE Trans. Ind. Appl.*, Vol.IA-20, No.2, pp.309–320 (1984)

(3) T-H. Liu, J.R. Fu, and T.A. Lipo: "A strategy for improving reliability of field oriented controlled induction motor drives", *IEEE Trans. Ind. Appl.*, Vol.29, No.5, pp.910–918 (1993)

(4) M.B. de R. Correa, C.B Jacobina, E.R.C. da Silva, and A.M.N. Lima: "An Induction Motor Drive System with Improved Fault Tolerance", IEEE Ind. Appl. Conf., Vol.4, pp.2071–2077 (2000)

(5) F. Blaabjerg, S. Freysson, H.H. Hansen, and S. Hansen: "A new optimized space-vector modulation strategy for a component-minimized voltage source inverter", *IEEE Trans. Power Electron.*, Vol.12, No.4, pp.704–714 (1997)

(6) F. Blaabjerg, D.O. Neacsu, and J.K. Pedersen: "Adaptive SVM to compensate DC-link voltage ripple for four switch three phase voltage source inverters", *IEEE Trans. Power Electron.*, Vol.14, No.4, pp.743–752 (1999)

(7) G.A. Covic and G.L. Peters: "DC link imbalance compensation in four switch inverter AC motor drives", Inst. Electr. Eng. Electron. Lett., Vol.33, pp.1011–1102 (1997)

(8) M.B. de R. Correa, C.B. Jacobina, E.R.C. da Silva, and A.M.N. Lima: "A general PWM strategy for four-switch three phase inverters", *IEEE Trans. Power Electron.*, Vol.21, No.6, pp.1618–1627 (2006)

(9) P.Q. Dzung, L.M. Phuong, H.H. Lee, and L.D. Khoa: "Dynamic adaptive space vector PWM for four switch three phase inverter fed induction motor with compensation of DC-link voltage ripple", Proc. 7th IEEE Int. Conf. Power Electron and Drive systems, pp.399–404 (2009)

(10) S. Kazemolu and M.R. Zolghadri: "Direct torque control of four switch three phase fed induction motor using a modified SVM to compensate DC-Link voltage imbalance", Int. Conf. Elect. Power and Energy Con. Syst., pp.1–6 (2009)

(11) R. Wang, J. Zhao, and Y. Liu: "A comprehensive investigation of four-switch three phase voltage source inverter based on double fourier integral analysis", *IEEE Trans. Power Electron.*, Vol.26, No.10, pp.2774–2787 (2011)

(12) P.Q. Dzung, L.M. Phoung,and P.Q. Vinh: "A new switching for direct torque control of induction motor using four-switch three-phase inverter", IEEE Int. Conf. Power Electron and Drive Syst., pp.1331–1336 (2007)

(13) J. Kim, J. Hong, and K. Nam: "A Current distortion compensation scheme for four-switch inverter", *IEEE Trans. Power Electron*, Vol.24, pp.1032–1040 (2009)

(14) P.Q. Dzung, L.M. Phuong, P.Q. Vinh, N.M. Hoang, and T.C. Binh: "New space vector control approach for four switch three phase inverter (FSTPI)", Proc. 7th Int. Conf. Power Electron and Drive Syst., pp.1002–1008 (2007)

(15) Q.T. An, L. Sun, K. Zhao, and T.M. Jahns: "Scalar PWM algorithms for four-switch three-phase inverters", IET Electronics Letters, Vol.46, pp.900–902 (2010)

(16) Y. Liu, X. Ge, J. Zhang, and X. Feng: "General SVPWM strategy for three different four switch three phase inverters", IET Electronics Letters, Vol.51, No.4, pp.357–359 (2015)

(17) W. Ma and M. Morimoto: "Emergency drive method for EV at the inverter fault", IEEE Int. Conf. on Elec. Machines and Syst. (ICEMS), pp.2008–2011 (2010)

(18) H. Tanaka, S. Saito, and K. Matsuse: "Improved performance of independent two induction motor drives fed by a four leg inverter with vector control method", IEEE Int. Conf. Elec. Machines and Syst. (ICEMS), pp.1–6 (2012)

(19) U.U. Ekong, M. Inamori, and M. Morimoto: "Field Oriented Control of two phase inverter to drive a three phase induction motor", IEEE int. Conf. on Elec. Machines and Syst. (ICEMS), pp.125–128 (2015)

Ufot Ufot Ekong (Student Member) was born in Lagos, Nigeria, in 1990. He received his B.Sc. and M.Sc. degree in electrical and electronic engineering from Tokai University Japan in 2014 and 2016. Presently, He is pursuing a Ph.D. degree at Tokai University. His research interests include power electronics and its applications, fault tolerant control and ac machines drives. He is a member of IEEE-IAS.

Mamiko Inamori (Member) was born in Kagoshima, Japan in 1982. She received her B.Sc., M.Sc. and Ph.D. degree in electronics engineering from Keio University, Japan in 2005, 2007 and 2009 respectively. In 2009, she joined Keio University where she was a lecturer. In 2013, she joined the Faculty of Engineering, Tokai University as a lecturer. Her research interests are mainly concentrated on power and communication systems.

Masayuki Morimoto (Fellow) was born in Tokyo, Japan in 1952. He received his B.Sc., M.Sc. and Ph.D. degree in electrical engineering from Keio University, Japan in 1975, 1977 and 1990 respectively. He worked at Mitsubishi Heavy Industries, Ltd. from 1977 to 2005. Since 2005, He has been a Professor at the Department of electrical and electronic engineering, Tokai University. His research interests are in the areas of power electronics and its applications, electric machines and drives, and vehicle application.